JOURNAL OF PHYSICAL ORGANIC CHEMISTRY, VOL. 10, 885–897 (1997)

AB INITIO THEORETICAL STUDY OF THE REACTIVITY AS BASES OR NUCLEOPHILES OF POTASSIUM AND LITHIUM METHIDES

GIOVANNI GHIGO[1], GLAUCO TONACHINI[1]* AND JACQUES FOSSEY[2]

[1] *Dipartimento di Chimica Generale e Organica Applicata dell' Università di Torino, Corso Massimo D'Azeglio 48, 10125 Turin, Italy*
[2] *École Polytechnique, DCMR, 91128 Palaiseau, France*

Using propene as a model reference system, the reactivity of potassium and lithium methides in metal–hydrogen exchange and nucleophilic addition to the double carbon–carbon bond was investigated. These extreme models, which imply a tight interaction of the organic anion with its counterion, were compared with the corresponding free anion reactions, which provide the opposite extreme situation. The lithium system appears to be more inclined toward nucleophilic addition, whereas the potassium system would more readily undergo a metallo-dehydrogenation reaction. The results appear to be consistent with available experimental evidence and allow a qualitative rationalization of the different basic strengths and nucleophilicities of Li and K alkyls. As an ancillary but interesting result, the hydrogen transfer reactions see a significant amount of electron density located on the transferred hydrogen in the transition structure; this process can hardly be defined as a proton abstraction operated by the strong base. © 1997 John Wiley & Sons, Ltd.

J. Phys. Org. Chem. **10**, 885–897 (1997) No. of Figures: 11 No. of Tables: 4 No. of References: 12

Keywords: potassium and lithium methods; reactivity; *ab initio* studies

Received 9 December 1996; revised 12 May 1997; accepted 12 May 1997

INTRODUCTION

On suitable substrates, nucleophilic addition to a multiple carbon–carbon bond and metallo-dehydrogenation can in principle compete. Metalation operates successfully if relatively acidic hydrogens can be involved. Addition generally occurs if the unsaturated substrate is activated, e.g. if the multiple CC bond is adjacent to a substituent capable of stabilizing a negative charge.[1] The same reactant (e.g. an alkali metal alkide) can perform as a metalating agent (a base) or a nucleophile, with the formation of a new carbon–carbon bond. For instance, α-dialkoxy-substituted β,γ-unsaturated systems have been found to behave differently with a simple alkyllithium reagent and in the simultaneous presence of a potassium cation (Scheme 1).[2] In the first case addition takes place, followed by elimination, with LiOR as leaving group. In the second case, a δ hydrogen is abstracted, with formation of an allyl–anionic system, followed again by an elimination step.

The main purpose in undertaking the present study was to compare the relative reactivities as bases or nucleophiles of potassium and lithium alkyls. In a first phase, two simple metallo-dehydrogenation reactions were examined. One is given by equations (1) and (2), in which an allylic carbanion

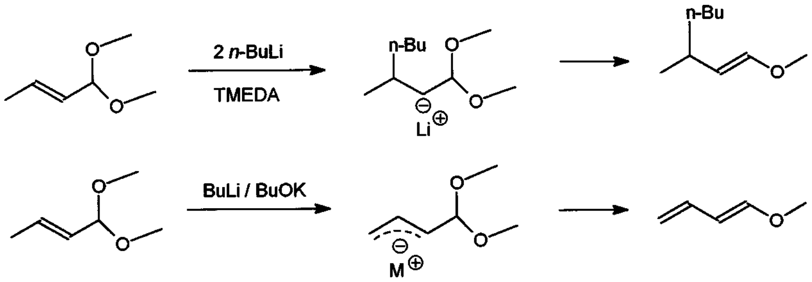

Scheme 1

---

* *Correspondence to:* G. Tonachini, Dipartimento di Chimica Generale e Organica Applicata dell'Università di Torino, Corso Massimo D'Azeglio 48, 10125 Turin, Italy.

Contract grant sponsor: CNR; *Contract grant number:* Bilateral Project 91.03502.03, registry No. 2264-3-91.

CCC 0894–3230/97/120885–13 $17.50

is formed.

$$CH_3^- K^+ + CH_3CH{=}CH_2 \rightarrow CH_4 + (CH_2CHCH_2)^- K^+ \tag{1}$$

$$CH_3^- Li^+ + CH_3CH{=}CH_2 \rightarrow CH_4 + (CH_2CHCH_2)^- Li^+ \tag{2}$$

The identity hydrogen exchange reactions in equations (3) and (4) provide a suitable extreme reference for carrying out a comparison with reactions (1) and (2). The acidity of the two alkyl hydrogens involved in the two sets of reactions is known to be very different, and is reflected by the experimental estimates of the relevant pK values.[3]

$$CH_3^- K^+ + CH_4 \rightarrow CH_4 + CH_3^- K^+ \tag{3}$$

$$CH_3^- Li^+ + CH_4 \rightarrow CH_4 + CH_3^- Li^+ \tag{4}$$

Although it is well known that organolithium compounds are most often present as oligomers,[4] the two reactions involving lithiated monomers were used with the purpose of carrying out a comparison with the analogous reactions involving potassium. Equation (4) had been already studied by Kaufmann and Schleyer,[5] who also reported interesting computational results relevant to the analogous reaction involving the methyllitium dimer.

The next step consisted in comparing the results relevant to the above equations with the related free anion models [equations (5) and (6)].

$$CH_3^- + CH_3CH{=}CH_2 \rightarrow CH_4 + (CH_2CHCH_2)^- \tag{5}$$

$$CH_3^- + CH_4 \rightarrow CH_4 + CH_3^- \tag{6}$$

The proton transfer reaction between carbon atoms in the methane–methide anionic system [equation (6)] had already been investigated by *ab initio* methods by Latajka and Scheiner.[6] The association of a carbanion with a metal cation yields a moiety whose nature is significantly affected by the nature of the counterion;[3] this comparison should assess if important differences in this interaction are present, in addition to the structural and electronic factors which bring them about.

Then, in a second phase, the relative inclination of lithium and potassium methide toward nucleophilic addition to a multiple carbon–carbon bond was studied by investigating the reactions shown in equations (7) and (8), which involve the same substrate used for the hydrogen exchange reaction, propene.

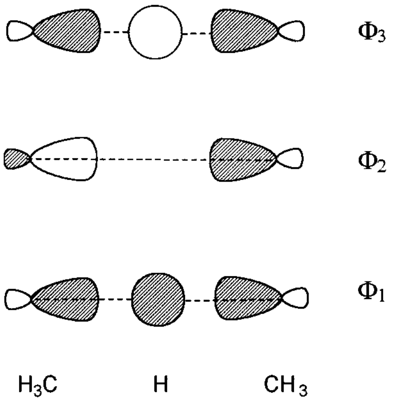

Figure 1. Active orbitals for the CAS–MCSCF calculations on the free anion transition structure

$$CH_3^- K^+ + CH_3CH{=}CH_2 \rightarrow CH_3C(CH_3)HCH_2^- K^+ \tag{7}$$

$$CH_3^- Li^+ + CH_3CH{=}CH_2 \rightarrow CH_3C(CH_3)HCH_2^- Li^+ \tag{8}$$

These were again compared with the analogous free anion reaction [equation (9)].

$$CH_3^- + CH_3CH{=}CH_2 \rightarrow CH_3C(CH_3)HCH_2^- \tag{9}$$

Nucleophilic addition reactions usually take place on activated substrates, as mentioned above,[1a] and were reported to require high temperatures on simple alkenes.[1b] For this reason, propene itself does not seem to offer a very realistic model for such an addition, although the structurally similar prop-2-en-1-ol molecule has been reported to give readily addition of *n*-butyllithium.[1c] Propene can thus be seen as an unreactive extreme case, nevertheless suitable for comparing the relative inclination of potassium vs lithium alkyls toward addition (in this sense the choice is similar to that of methane, an extremely weak acid, for studies of metallo-dehydrogenation). Moreover, it allows one to compare the result so obtained with that relevant to the metallo-dehydrogenation reaction occurring on the same system. Thus, propene can provide a single reference to assess on a relative basis the inclination of potassium and lithium alkyls toward the two reactions.

Solvation is an additional and very important factor,[3] in that it affects the very nature of the species investigated, by determining the balance between the different forms of association at equilibrium, which can range from intimate ion pairs to the separately solvated ions (for lithium alkyls it also affects the degree of aggregation into oligomers). However, only the two extreme model situations just mentioned will be examined here, and the explicit effects of solvation on the metallo-dehydrogenation process will be explored in a subsequent paper.

The Results and Discussion section is in two parts. In the first, the identity (metal–)hydrogen exchange reactions [equations (3), (4) and (6)] are examined, (i) to define clearly the nature of the wavefunction in the transition structures and (ii) to set a reference for the metallation reactions of propene. In the second part, the hydrogen abstraction [equations (1), (2) and (5)] and addition [equations (7), (8) and (9)] reactions involving propene are discussed.

METHOD

The study of the model reactions was performed by determining on the energy hypersurface the critical points relevant to stable and transition structures. This was accomplished by way of complete gradient optimization[7] of the geometrical parameters at the CAS–MCSCF[8] (for the identity metallo-dehydrogenation reactions) and MP2[9a] (for all reactions) levels of theory, using an sp split-valence shell basis set by Huzinaga *et al.*,[10a] enriched with diffuse p functions and d polarization functions on C and p polarization functions on Li and K, hereafter referred to as [53/331/31/2].[10b] For the reactions involving propene, the study at the MP2 level was preceded by the determination of the critical points at the monodeterminantal level; these were then characterized as minima or first-order saddle points through diagonalization of the analytically calculated Hartree–Fock Hessian matrix (vibrational frequencies calculation). In the figures in the following section, the reported interatomic distances are in ångströms and angles in degrees (dihedral angles in parentheses). The MP2/[53/331/31/2] geometries were then used to recompute the relative energies at the MP3 and MP4 levels,[9a] and also through coupled cluster calculations, at the CCSD(T) level,[9b] using the same basis set. The electron distribution was examined in terms of NAO charges (natural population analysis).[11] The Gaussian92 system of programs[12] was used throughout on IBM RISC/6000-550 and 360 computers at the Dipartimento di Chimica Generale e Organica Applicata.

RESULTS AND DISCUSSION

Identity metal–hydrogen exchanges

CAS-MCSCF study

A preliminary investigation of the transition structures (TS) for the identity reactions [equations (3), (4) and (6)] was first carried out at a multi-configurational level of theory, in order to assess if the monodeterminantal level of theory is able to provide a qualitatively correct picture of this process in the more complex systems. The active space in the CAS–MCSCF calculations thus undertaken includes, for the neutral systems, four orbitals, in which four electrons are placed in every possible way (complete CI). In the simpler

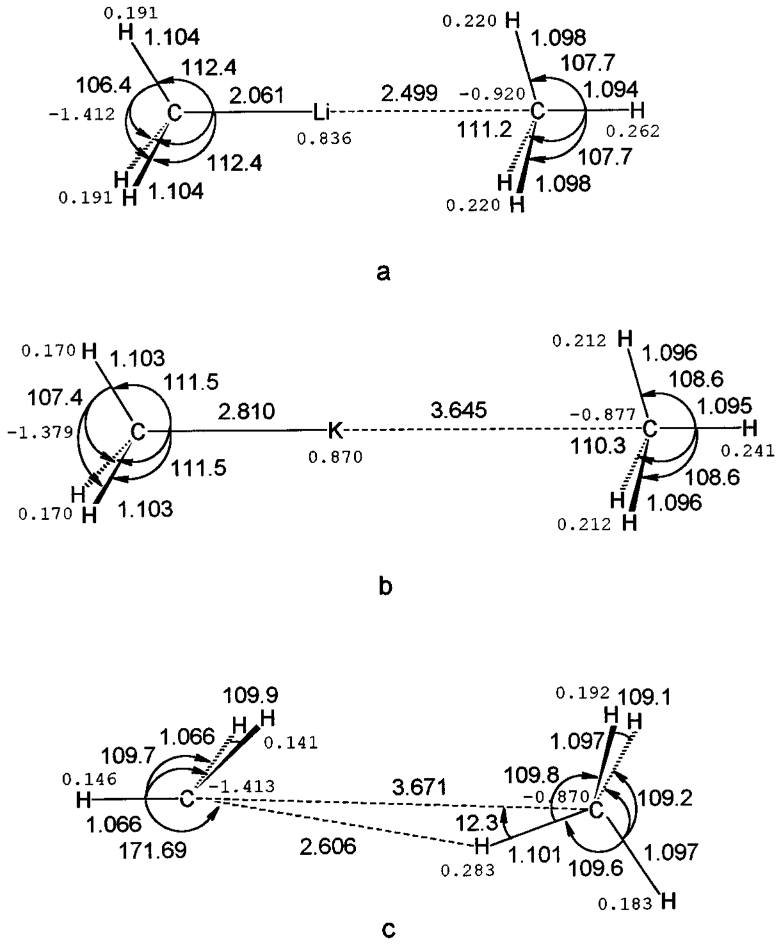

Figure 2. The ion–dipole complexes

case of the anion, the three molecular orbitals which can be found at the symmetric transition structure geometry are as depicted in Figure 1.

The analysis of the CAS–MCSCF wavefunction of the optimized structures provides two main results. (i) The molecular orbitals resulting from the MCSCF procedure, delocalized over the whole system, have an electron occupation either close to 2 or to zero, and the aufbau configuration is dominant in the CI eigenvector (with coefficient 0·99 for all transition structures). Hence no diradical character appears to be present in the wavefunction corresponding to these structures. (ii) A significant electron density is found on the migrating hydrogen, and originates principally from its participation in the Φ_1 orbital (it would therefore not be appropriate to see the process as a proton transfer). Ancillary information on the role of the metal cation is provided by this series of computations. In this case, the four active orbitals (not shown) present only small contributions from the cation empty orbitals, thus confirming that its role is limited to electrostatic interaction with the rest of the system. Therefore, it can be safely concluded that the study of the energy hypersurfaces for these reactions either at the monodeterminantal level or at a perturbative (MP2) level based on a single reference can be qualitatively correct.

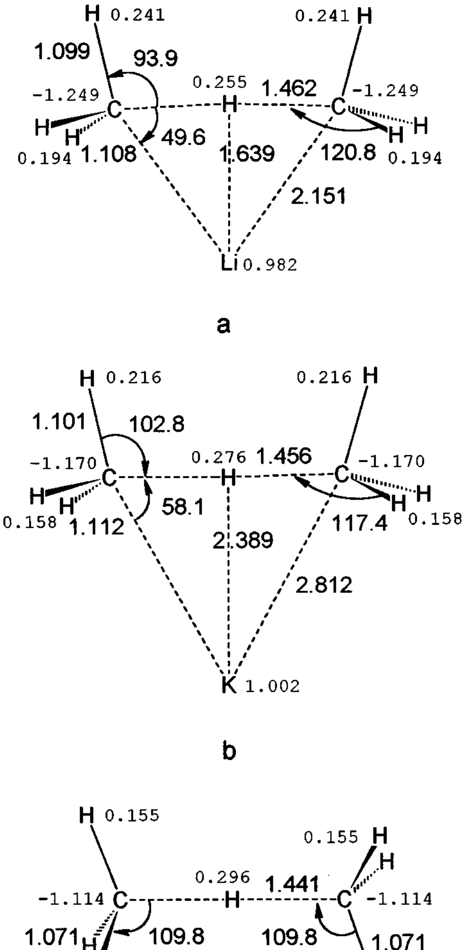

Figure 3. Hydrogen exchange transition structures for the (a) lithiated, (b) potassiated and (c) free-anion systems

Møller–Plesset and coupled cluster calculations

Reactions (3) and (4) were then studied at the MP2 level and compared with reactions (6). Unconstrained optimization of the ion–dipole complexes for the lithium and potassium systems resulted in the two simple and similar structures shown in Figure 2(a) and (b). In the case of the free anion, a structure more asymmetric than expected was found [Figure 2(c)].

The transition structure for the hydrogen–potassium exchange between two methyl groups is shown in Figure 3(b). Those determined at the same computational level for the lithiated and free-anion systems [Figure 3(a) and (c)] are reported here for sake of comparison, although already studied by other researchers.[5, 6]

The anionic part of the metallated systems resembles the transition structure of the free anion reaction; the two carbons and the migrating hydrogen are almost collinear, and the migrating hydrogen–carbon distance value is slightly increased, more in Figure 3(a) than in Figure 3(b). The metal cation thus appears to interact with the rest of the system with modest perturbation of the geometry (mainly some clockwise and anti-clockwise rotation of the two methyls), which allows a better interaction among the cation and the two carbons. The C—Li distance in Figure 3(a) undergoes a lengthening of +0·090 Å, indicating that the carbon–lithium interaction is still significant, although not allowed to develop at its best. In contrast, the C—K distance in Figure 3(b) is virtually unmodified; this is most likely due to the already long distance between the negative carbon and potassium in the complex, which puts less stringent requirements on the geometrical changes necessary to accommodate for two C–K interactions. On the other hand, the H—Li and H—K distances appear to be rather short.

The RHF NAO charges,[11] shown in Figure 3 as smaller numerals, show that the transferred H is associated to a significant electron density. Electron density (ρ) maps, corresponding to a cut on the plane containing the two carbons, the migrating hydrogen, and the cation confirm this description. The ρ map relevant to Figure 3(b) is reported in Figure 4 as an example.

As regards the energetics of these reactions, the convergence of the perturbative treatment was checked by way of calculations carried out at the MP3, MP4 and coupled cluster [CCSD(T)] levels of theory. The data reported in

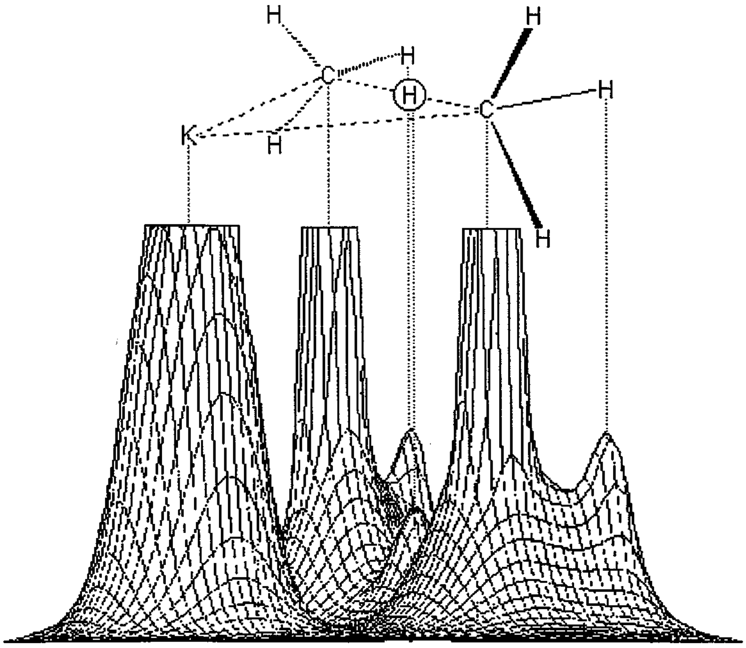

Figure 4. Electron density map on the KCC plane relevant to the transition structure in Figure 3(b). The transferred hydrogen (circle) lies on the same plane

Table 1 show that the convergence of the computed energy differences is satisfactory.

Table 1. Energy barriers[a] for the identity hydrogen–metal exchange reactions

Theory level[b]	E (complex)	E (transition structure)	$\Delta E^{\ddagger}$
Li:	Figure 2(a)	Figure 3(a)	
CCSD(T)//MP2	− 87·454075	− 87·396469	36·1
MP4//MP2	− 87·451910	− 87·394985	35·7
MP3//MP2	− 87·438720	− 87·381071	36·2
MP2//MP2	− 87·408590	− 87·353518	34·6
K:	Figure 2(b)	Figure 3(b)	
CCSD(T)//MP2	− 678·525635	− 678·482689	26·9
MP4//MP2	− 678·523160	− 678·481062	26·4
MP3//MP2	− 678·508938	− 678·466721	26·5
MP2//MP2	− 678·480027	− 678·439146	25·7
Anion:	Figure 2(c)	Figure 3(c)	
CCSD(T)/MP2	− 79·960720	− 79·935295	16·0
MP4//MP2	− 79·958758	− 79·933375	15·9
MP3//MP2	− 79·943797	− 79·917568	16·5
MP2//MP2	− 79·915684	− 79·891604	15·1

[a] In kcal mol^{-1} (1 kcal = 4·184 kJ); computed with respect to the electrostatic complexes in Figure 2; total energies in hartree.

[b] Coupled cluster and Møller–Plesset single-point energy calculations using the [53/331/31/2][10] basis set, carried out on the MP2/[53/331/31/2] optimum geometries.

Interpretation of the observed trends

It can be seen from Table 1 that the ordering of the activation barriers is $\Delta E^{\ddagger}(\mathrm{Li}) > \Delta E^{\ddagger}(\mathrm{K}) > \Delta E^{\ddagger}$ (anion). This ordering can be related to the different destabilization of the bonding situation of the reactant complexes, as the geometry of the systems departs from its optimum arrangement in Figure 2(a)–(c); owing to the symmetry of these systems, the same destabilization occurs when proceeding backwards from the identical products. Taking the anion situation as a reference ‘baseline’, attention can be focused on the differences in destabilization which can occur if a metal cation is present. The observed trend can be due to the interplay of two component energetic effects: the first (labeled D) is related to a deformation of the geometries with respect to those found in the anionic system, i.e. elongation of the migrating hydrogen–carbon bond, deformation and reorientation of the two methyl groups, and the second (labeled S) to the metal cation–anionic system stabilizing interaction (Scheme 2).

The starting reference point for this analysis is provided by the energy of the two separated moieties CH_3^- and CH_4 (Scheme 2, left end of the upper curve). At the geometries in Figure 2(a) and (b), the CH_3^- and CH_4 moieties are held together by their interaction with M^+, but their distance is large and their mutual interaction tiny. This allows one to

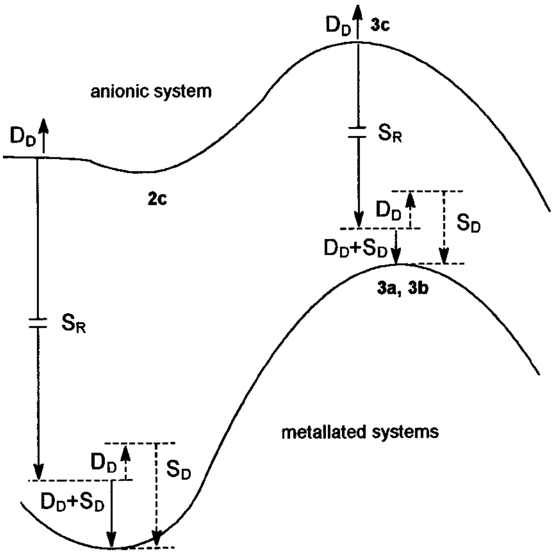

Scheme 2

choose the two separated fragments as a reference, and not the complex in Figure 2(c) [the presence in this complex of interactions which are absent in Figure 2(a) and (b) would make its choice as a reference more arguable]. If the deformation-destabilizing contribution for the separated CH_3^- and CH_4 optimized moieties is defined as zero ($D=0$), and the three moieties are brought together at the C—M distances shown in Figure 2(a) and (b) while keeping the geometries of the separated fragments frozen, then an electrostatic 'stabilization with rigid geometries' (S_R) can be defined and evaluated. Further stabilization can be achieved by the metallated system by relaxing the geometry to obtain that in Figure 2(a) or (b), for which the energy is already available. However, the stabilization so calculated is in fact made up of two different contributions: (1) the metal cation–anionic system stabilizing interaction is optimized by orienting and deforming to some limited extent the CH_3^- and CH_4 moieties; and (2) this same deformation brings about a modest destabilization of the anionic part of the system. These two distinct effects can be named S_D ('stabilization resulting from a deformation') and D_D ('destabilization resulting from a deformation'). The further energy lowering, calculated by comparing the energies of the rigid complex and that of the optimized complex, is thus given by D_D+S_D. The destabilization D_D can be evaluated separately, by deforming the CH_3^- and CH_4 species in the absence of M^+ (indicated by D_D and the upwards arrow in the leftmost part of the upper curve, Scheme 2). The estimate of D_D can subsequently be reported in the lower

Table 2. Energy contributions[a] to the differences in barrier height in the hydrogen–metal exchange identity reactions

	Complex		Transition structure				
	S_T	D_D	S_T	D_D	ΔS_T	ΔD_D	$\Delta\Delta E^‡$
Li	−172·5	1·1	−156·2	6·9	16·3	5·8	22·1
K	−121·2	0·4	−109·8	2·2	11·4	1·8	13·2

[a] In kcal mol^{-1}; computed at the MP2/[53/331/31/2] level.

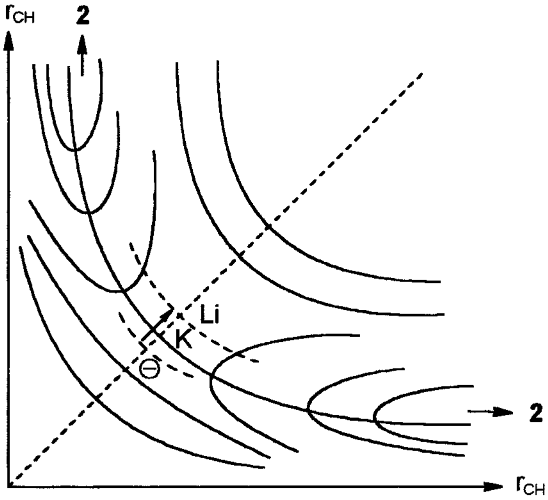

Figure 5. Overview of a three-dimensional cut of the potential energy hypersurface for the identity reactions; r_{CH} denotes the distances between the migrating hydrogens and one of the two carbons

left part of Scheme 2 to dissect conceptually the sum $D_D + S_D$ into its two components (dashed arrows). The overall stabilization originating from the metal cation–anionic system interaction is thus given by $S_T = S_R + S_D$, in which the S_R term is largely dominant.

The same dissection scheme can now be set up for the transition structures, with the anionic one providing a suitable reference (Scheme 2, right). If the anionic structure in Figure 3(c) is deformed to a geometry such as that in Figure 3(a) or (b), a destabilization D_D can be evaluated. Similarly, S_R and $D_D + S_D$ contributions can be computed by rigidly assembling the anionic transition structure and the metal cation (S_R), and then comparing with the energies of the structures in Figure 3(a) or (b), already available. D_D can again be reported to single out the S_D contribution, and then estimate S_T (dashed arrows). Having at this point collected the S_T values for Li and K in both the complexes and transition structures, the loss of metal cation–anionic system

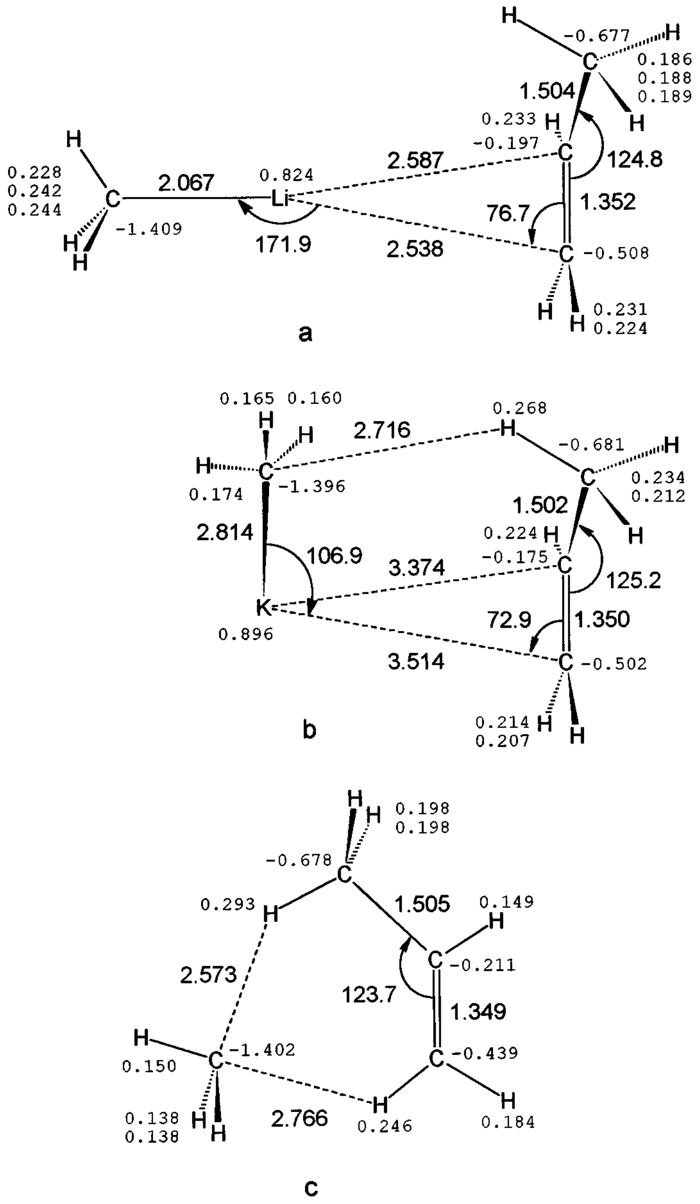

Figure 6. Ion–dipole complexes for the (a) lithiated, (b) potassiated and (c) free-anion methide–propene systems

stabilizing interaction, ΔS_T, can be calculated.

The values reported in Table 2 show that (i) S_T is larger for the lithium system, in both the complex and the transition structure (consistent with the relevant geometrical features); (ii) a larger ΔS_T is observed in the lithium case, on going from the complex to the transition structure; (iii) a larger change in destabilization due to deformation, ΔD_D, is found again for the lithium case (this appears to be consistent with the shorter C—M$^+$ distances); and (iv) both ΔS_T and ΔD_D concur to give a higher barrier for the lithiated system: the former effect is larger, but the latter is not unimportant, especially for lithium. In other words, in the case of lithium, the transition structure is more deformed than in the case of potassium (anion as a reference) but, in spite of that, is less stabilized by the cation. The fact that the saddle point on the energy hypersurface is reached only

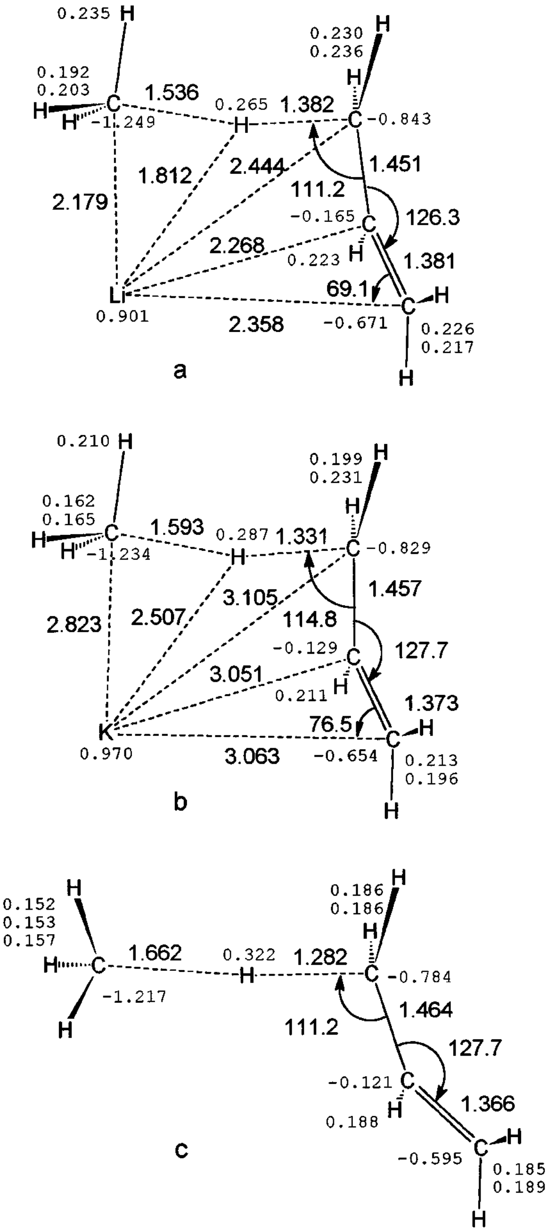

Figure 7. H-exchange transition structures for the (a) lithiated, (b) potassiated and (c) free-anion methide–propene systems

corresponding to a larger elongation of the C—H bond (arrow in Figure 5) can be interpreted as a consequence of the features just discussed.

Metallo-dehydrogenation of propene

The system resulting from the metallo-dehydrogenation reactions (1) and (2) is an allylic system: this provides a stabilization which is not present in the simpler cases discussed in the previous section (p*K* values are estimated to differ by 10 orders of magnitude).[3] The negative charge is spread out on a relatively large system, and its interaction with the cation changes along the reaction path in a different way with respect to the methide–methane systems, possibly assuming a different importance in the lithium and potassium cases.

The electrostatic complexes are shown in Figure 6. A difference between Figure 6(a) and (b) is evident. In the former, only lithium interacts with propene, and methide is opposite to it, providing a linear arrangement of the negative carbon, the cation and the midpoint of the double bond. In the latter, possibly because of a weaker methide–potassium interaction, the negative carbon is able to establish some interaction with a methyl hydrogen of propene, and the resulting structure is bent. Two interactions are present also in the complex in Figure 6(c), in which the negative carbon is fairly close to two propene hydrogens. The real importance of these structural differences is most likely to be very limited, because these gas-phase models lack, among other things, the coordination saturation of the cation by solvent molecules. However, these complexes provide a suitable reference to discuss qualitatively the trends in barrier heights, which is the goal of this study.

The transition structures are displayed in Figure 7. Comparison of some interatomic distances with the complexes in Figure 6(a) and (b) reveals some interesting trends. The interaction of the metal cation with the methide carbon is diminished: the variation in the C—Li distance amounts to +0.112 Å, whereas for potassium this effect is limited to +0.009 Å (as was the case for the identity reaction). At the same time, the attraction of both lithium and potassium for the double bond carbons is strengthened in the structures in Figure 7(a) and (b), the cation–carbon distances decreasing to *ca* 90% of their values in the complexes. This effect is expected, because these two carbons, in addition to the propene methyl carbon, are becoming part of an allyl anion system. In fact, the

Table 3. Energy barriers[a] for the hydrogen–metal exchange and addition reactions of propene[b]

		H-exchange		Addition	
Theory level[c]	*E* (complex)	*E* (transition structure)	$\Delta E^{\ddagger}$	*E* (transition structure)	$\Delta E^{\ddagger}$
Li:	Figure 5(a)	Figure 6(a)		Figure 7(a)	
CCSD(T)//MP2	−164·540260	−164·500527	25·1	−164·507410	20·6
MP4//MP2	−164·537214	−164·498768	24·1	−164·505919	19·6
MP3//MP2	−164·510332	−164·468753	26·1	−164·475151	22·1
MP2//MP2	−164·466531	−164·431133	22·2	−164·436294	19·0
K:	Figure 5(b)	Figure 6(b)		Figure 7(b)	
MP4//MP2	−755·605730	−755·583555	13·9	−755·578957	16·9
MP3//MP2	−755·577791	−755·553429	15·3	−755·547499	19·0
MP2//MP2	−755·535077	−755·515190	12·5	−755·508533	16·7
Anion	Figure 5 (c)	Figure 6(c)		Figure 7(c)	
CCSD(T)//MP2	−157·043024	−157·032840	6·4	−157·031024	7·5
MP4//MP2	−157·040065	−157·030923	5·7	−157·029046	6·9
MP3//MP2	−157·011028	−157·000071	6·9	−156·996487	9·1
MP2//MP2	−156·969402	−156·962163	4·5	−156·958892	6·6

[a] In kcal mol^{-1}; computed with respect to the electrostatic complexes in Figure 5; total energies in hartree.

[b] MP2/[53/331/31/2] product energies: (1) dehydrogenation (allyl system plus methane; methane energy, −40·294058, added in): −164·478477 (Li), −755·560283 (K), −157·003473 (anion); (2) addition (isobutyl system): −164·488668 (Li), −755·566024 (K), −157·004258 (anion).

[c] Coupled cluster and Møller–Plesset single-point energy calculations using the [53/331/31/2][10] basis set, carried out on the MP2/[53/331/31/2] optimum geometries.

variations in the two C—C bond lengths of propene show that in Figure 7(a) the two bonds are shortened and stretched by 56% and 51%, respectively, of the total variation necessary to attain the symmetric geometry of allyllithium; in Figure 7(b) by 47% and 40% and in Figure 7(c) only by 40% and 31%. The deformation of the propene part of the systems is thus substantial and develops to a larger extent in the order Li > K > anion.

The transition structures in Figure7(a)–(c) exhibit, from the point of view of the hydrogen transfer process, a relative earliness, or facility, with respect to the identity reactions (compare Figure 3). The earliness increases, in the series of structures in Figure 7(a)–(c), following the order anion- > K > Li.

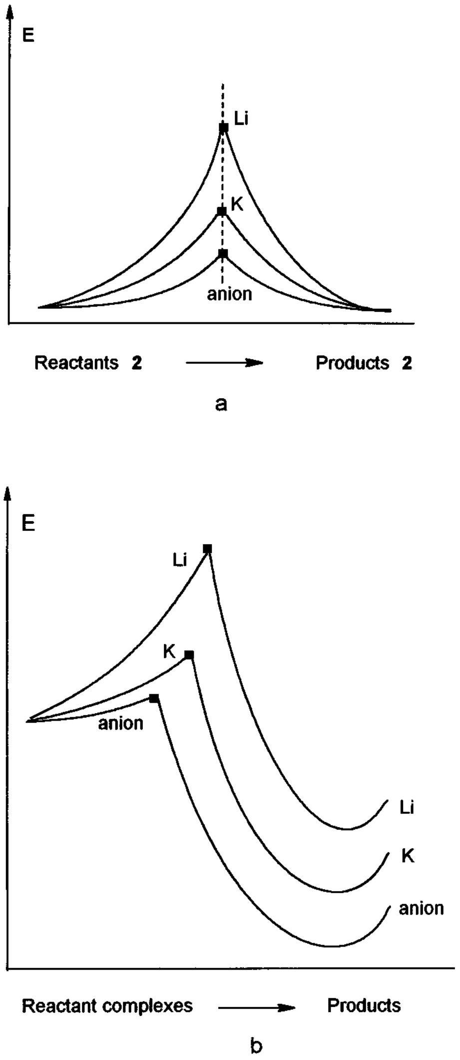

Figure 8. Qualitative sketch of the intended crossings between three pairs of ascending reactant curves and descending product curves (exothermicity factor) for the lithiated, potassiated and free-anion methide–propene systems

In a parallel way, the energy barriers with respect to the complexes (Table 3) become lower on going from lithium to potassium and finally to the anionic system. Two main factors can be thought of as concurring with the trend in barrier heights and the relative earliness of the relevant transition structures. The first is the different destabilization of the bonding situation of the reactant system as the reaction proceeds and the nuclei gradually rearrange. This part parallels what was already seen for the identity reactions, where this was the only contribution ($\Delta E_{\text{reaction}} = 0$); in Table 2 it was dissected into two distinct contributions, ΔD_{D} and ΔS_{T}. The second factor is the exothermicity of the process considered. This attempt to rationalize the computed trends is sketched in Figure 8. The different steepnesses of the three ascending curves on the left can again be related to a larger geometrical deformation of the hydrocarbon groups. These curves are, in order of increasing slope, that for the anion, that for potassium and that for lithium. Deformation is accompanied by a partial loss of stabilizing anion–cation interaction, particularly effective in the lithium case. In fact, while the interaction with methide is diminished only in the lithium structure in Figure 7(a), the interaction with the other carbons is approximately increased to the same extent for both cations. In the identity reactions, the larger these factors, the longer was the transferred hydrogen–carbon distance. However, in the present case, the exothermicity factor must also be considered. The delocalization of the negative charge attained in the products of reactions (1), (2) and (5) has a twofold consequence. All three reactions are exothermic (footnote c in Table 3); the energy difference between the products (structures not shown) and the reactant complexes, computed at the MP2/[53/331/31/2] level of theory only, are $-7{\cdot}5$ (Li), $-15{\cdot}8$ (K) and $-21{\cdot}4$ kcal mol^{-1} (anion). In other words, the allylic anionic system (with or without counterion) plus methane is more stable than propene plus methide (with or without counterion), as associated in the structures in Figure 6. However, the delocalization of the negative charge attenuates the stabilizing interaction with the cation, especially in the lithium case, where the interaction with methide is more effective. The main geometrical parameters of the propene hydrogen exchange

Table 4. Geometrical parameters of propene hydrogen exchange products[a]

	Li	K	Anion
C—C	1·409	1·407	1·403
<CCC	126·7	129·6	131·4
M^+—C_β	2·153	2·900	—
M^+—$C\alpha, \gamma$	2·183	2·928	—

[a] Bond lengths in Å, angles in degrees.

products, allyl anion and its metallated derivatives, are reported in Table 4. In the products the distances between lithium and the two terminal carbons of the allylic group are 0·116 Å longer than that in $LiCH_3$ [in Figure 6(a)] and that for potassium is 0·114 Å longer than that in KCH_3 [in Figure 6(b)]. Thus, the free anion system shows the largest exothermicity and the lithiated system the lowest. The destabilization factor alone would seem to be capable of explaining the trend in barrier heights (Figure 8); the $\Delta E^{\ddagger}$ increments in the lithium, potassium and anion series (8–10 kcal mol^{-1}) are similar to those found in the identity reactions (*ca* 10 kcal mol^{-1} each). It can be noted, however, that exothermicity lowers the barriers with respect to the identity reactions, as expected. Moreover, only the interplay of both destabilization and exothermicity factors can suggest a rationale for the trend regarding the earliness of the transition structures (the position of the transition structure along the reaction coordinate is here assumed to be approximately determined by the avoided crossing region). In Figure 8, the black squares mark the intended crossing regions, related to the earlier or later occurrence of the transition structures on the reaction pathway. It is apparent that the larger or smaller exothermicity can have a direct influence on the position of the crossing point. The earlier the transition structure, the shorter is the stretch of reaction pathway along the ascending curve actually followed by the system, and the lower, in turn, is the overall deformation undergone by the reacting system at that point of the reaction pathway. Reactant destabilization is thus allowed by exothermicity to develop to a smaller extent for the anion than for the potassium system, and is the largest for the lithium system; this effect cooperates with the different slopes of the destabilized reactant curves on the left in Figure 8, which in this case follow the same order. Exothermicity thus intervenes in what could be denoted an *intrinsic* potential destabilization for each system, prone to grow more or less promptly as the nuclei rearrange, and determines the *actual* destabilization developed at the crossing point.

In summary, all transition structures for the propene hydrogen exchange reactions are earlier than those found for the identity reactions and more easily attained in terms of energy; the earliest is that for the anionic system [Figure 7(c)] to which the lowest barrier corresponds, followed in the order by those involving potassium [Figure 7(b)] and lithium [Figure 7(a)]. Both aptitude toward destabilization shown by the reactants and product stability concur to define these trends.

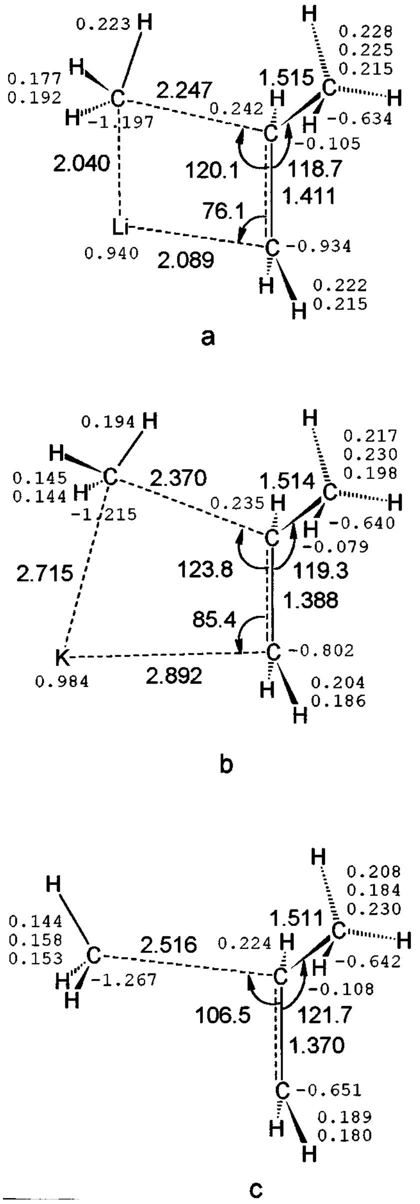

Figure 9. Addition transition structures for the (a) lithiated, (b) potassiated and (c) free-anion methide–propene systems

Addition to the double bond in propene

The energy barriers for reactions (7)–(9) are referred, in Table 3, to the same initial complexes [Figure 6(a)–(c)] considered in the previous subsection. As for the previous reaction, the barriers decrease in the series lithium, potassium, anion. If these figures are compared in each case with those relevant to the metalation barriers, it appears that the lithium methide–propene system will prefer an addition pathway, whereas the analogous potassium system will be more inclined to undergo a metallo-dehydrogenation reaction.

The transition structures are shown in Figure 9. Again, the three structures display differences in the main geometrical parameters which allow one to classify the structure in Figure 9(a) as later and that in Figure 9(c) as earlier, with that in Figure 9(b) in the middle. For instance, the distances between the methide carbon and the attacked double bond carbon show increments of 0·12 Å on going from Figure 9(a) to (b), and 0.15 Å from Figure 9(b) to (c), respectively. Conversely, the double bond lengthening is more pronounced in Figure 9(a) than in (b) and in Figure 9(b) than in (c).

The exothermicities with respect to the reactant complexes in Figure 6 (from MP2/[53/331/31/2] optimizations) are $-13{\cdot}9$ (Li), $-19{\cdot}4$ (K) and $-21{\cdot}9$ kcal mol^{-1} (anion). The last value is not very different from that calculated for the hydrogen exchange reaction, but the first two are larger. With the anionic product as a reference, lithium appears to be more effective in stabilizing the localized isobutyl anion than the allyl system (by 6·4 kcal mol^{-1}); the same can be said of potassium, but the effect is smaller (3·6 kcal mol^{-1}). The trend is qualitatively the same as observed in the previous subsection, but the larger exothermicity found here for lithium seems to affect to some extent the barrier height. Thus, while the barriers to addition are higher than those for hydrogen exchange in the anionic and potassium systems, the reverse is true for lithium.

ACKNOWLEDGEMENTS

Financial support from the Italian CNR (within the Bilateral Project 91·03502·03, registry No. 2264-3-91) is gratefully acknowledged. The IBM RISC-6000/550 computer was provided to G.T. by the Italian CNR within the project 'Calcolo Avanzato in Chimica.'

REFERENCES

1. (a) Effective substituents are, for instance, second-row elements such as sulfur, carbonyl or cyano groups or other conjugated multiple bonds (Michael-type reactions). Also alkenes with an electron donor group in a suitable position (such as allylic alcohol, see below):

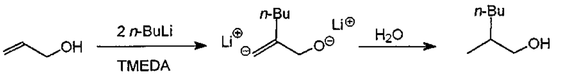

have been reported to undergo readily addition of organolithiums. See: B. J. Wakefield, in *Organolithium Methods*, Chap. 4. Academic Press, New York (1990); (b) H. E. Podall and W. E. Foster, *J. Org. Chem.* **23**, 1848–1852 (1958); (c) J. K. Crandall and A. J. Rojas, *Org. Synth.* **55**, 1–3 (1976); (d) M. Nakamura, E. Nakamura, N. Koga and K. Morokuma, *J. Chem. Soc., Faraday Trans.* **90**, 1789–1798 (1994); E. Nakamura, M. Nakamura, Y. Miyachi, N. Koga and K. Morokuma, *J. Am. Chem. Soc.* **115**, 99–106 (1993); E. Nakamura, Y. Miyachi, N. Koga and K. Morokuma, *J. Am. Chem. Soc.* **114**, 6686–6692 (1992).
2. (a) See, for instance: M. Schlosser, *Mod. Synth. Methods* **6**, 227–278 (1992); A. Mordini, in *Advances in Carbanion Chemistry*, edited by V. Snieckus, Vol. 1, p. 1. JAI Press, Greenwich, CT (1992); J. Fossey, G. Ghigo, G. Tonachini, P. Venturello, *Tetrahedron* **53**, 7937–7946 (1997); (b) The theoretical study of the reactivity modes of Schlosser's LICKOR superbase, carried out by considering the intervention of different aggregates and their structural and electronic features, suggests that the alkide reactant moiety is likely to act as a loose potassium alkide molecule, with a K$^+$—C$^-$ distance of *ca* 3·02 Å, instead of the more usual 2·88–2·89 Å; G. Ghigo, G. Tonachini and P. Venturello, *Tetrahedron* **52**, 7053–7062 (1996).
3. A p*K* of *ca* 43 is estimated for propene in LiCHA–CHA: D. W. Boerth and A. Streitwieser, Jr, *J. Am. Chem. Soc.* **103**, 6443–6447 (1981); a value ranging from 47 to 48 in THF–HMPA was also estimated: B. Jaun, J. Schwarz and R. Breslow, *J. Am. Chem. Soc.* **102**, 5741–5748 (1980). The p*K* value for methane was extrapolated from toluene and diphenylmethane: the estimate ranges from 52 to 62 (same reference). For a discussion on the acidity of hydrocarbons see, for instance: F. A. Carey and R. J. Sundberg, *Advanced Organic Chemistry*, Chapt. 7. Plenum Press, New York, (1990).
4. For the oligomerization of alkyllithiums, see: E. Kaufmann, J. Gose and P. v. R. Schleyer, *Organometallics* **8**, 2577–2584 (1989); E. Kaufmann, K. Raghavachari, A. E. Reed and P. v. R. Schleyer, *Organometallics* **7**, 1597–1607 (1988), and references cited therein. Here MeLi is just considered as a simple model for a generic alkyl group, and aggregation problems are plainly neglected. Not all alkyllithium have a strong inclination to aggregate: bulky *t*-BuLi, for instance, has been shown to exist as a monomer in tetrahydrofuran: W. Bauer, W. R. Winchester and P. v. R. Schleyer, *Organometallics* **6**, 2371–2379 (1987). Theoretical studies carried out in this laboratory indicate that changing the structure of the anionic moiety by introduction of heteroatoms (Y) significantly affects the anion–cation interactions which determine the tendency to give aggregates; see, for Y = F, C. Canepa, P. Antoniotti and G. Tonachini, *Tetrahedron* **50**, 8073–8084 (1994), and, for Y = Cl, C. Canepa and G. Tonachini, *Tetrahedron* **50**, 12511–12520 (1994).
5. E. Kaufmann and P. v. R. Schleyer, *J. Comput. Chem.* **10**, 437–448 (1989). In this study groups other than methyl (H, NH$_2$, OH, F) were also considered. A related study was carried out on the reaction of LiH with methane and acetylene (whose hydrogens exhibit a very different acidity); these reactions were found to proceed through four center transition structures, with very different activation barriers: E. Kaufmann, S. Sieber and P. v. R. Schleyer, *J. Am. Chem. Soc.* **111**, 121–125 (1989).
6. Z. Latajka and S. Scheiner, *Int. J. Quantum Chem.* **29**, 285–292 (1986).
7. H. B. Schlegel, in *Computational Theoretical Organic Chemistry*, edited by I. G. Csizsmadia and R. Daudel, p. 129. Reidel, Dordrecht (1981); H. B. Schlegel, *J. Chem. Phys.* **77**, 3676–3681 (1982); H. B. Schlegel, J. S. Binkley and J. A. Pople, *J. Chem. Phys.* **80**, 1976–1981 (1984); H. B. Schlegel, *J. Comput. Chem.* **3**, 214–218 (1982).
8. M. A. Robb and R. H. A. Eade, *NATO Adv. Study Inst. Ser.* **C67**, 21 (1981).
9. (a) C. Møller and M. S. Plesset, *Phys. Rev.* **46**, 618 (1934); J. S. Binkley and J. A. Pople, *Int. J. Quantum Chem.* **9**, 229–236 (1975); J. A. Pople, J. S. Binkley and R. Seeger, *Int. J. Quantum Chem. Symp.* **10**, –19 (1976); R. Krishnan and J. A. Pople, *Int. J. Quantum Chem.* **14**, 91–100 (1978); (b) J. A. Pople, R. Krishnan, H. B. Schlegel and J. S. Binkley, *Int. J.*

Quantum. Chem. **14**, 545–560 (1978); G. D. Purvis and R. J. Bartlett, *J. Chem. Phys.* **76**, 1910–1918 (1982); G. E. Scuseria, C. L. Janssen and H. F. Schaefer, III, *J. Chem. Phys.* **89**, 7382–7387 (1988); G. E. Scuseria and H. F. Schaefer, III, *J. Chem. Phys.* **90**, 3700–3703 (1989); see also: R. J. Bartlett, *Annu. Rev. Phys. Chem.* **32**, 359–401 (1981) for a discussion on these two methods and their performances.

10. (a) S. Huzinaga, J. Andzelm, M. Klobukowski, E. Radzio-Andzelm, Y. Sakai and H. Tatewaki, in *Physical Sciences Data*, Vol. **16**. Elsevier, Amsterdam (1984); (b) the basis consists, for K/C/Li/H, of (13s, 8p/7s, 5p, 1d/7s, 1p/4s) gaussians, respectively. These are grouped as 43321 (s) and 431 (p, the last one acting as a polarization set) for K, 421 (s), 311 (p, the last one a diffuse functions set) and 1 (d, a polarization set) for C, 421 (s) and 1 (p, a polarization set) for Li and 31 (s) for H. This grouping provides a [53/331/31/2] basis set, which is triple-ζ quality in the valence shell.
11. A. E. Reed, R. B. Weinstock and F. Weinhold, *J. Chem. Phys.* **83**, 735–746 (1985).
12. M. J. Frisch, G. W. Trucks, M. Head-Gordon, P. M. W. Gill, M. W. Wong, J. B. Foresman, B. G. Johnson, H. B. Schlegel, M. A. Robb, E. S. Replogle, R. Gomperts, J. L. Andres, K. Ragavachari, J. S. Binkley, C. Gonzales, R. I. Martin, D. J. Fox, D. J. Defrees, J. Baker, J. J. P. Stewart and J. A. Pople, *Gaussian92*. Gaussian, Pittsburgh, PA (1992).